

Colossal electroresistance in the ferromagnetic insulating state of single crystal  $\text{Nd}_{0.7}\text{Pb}_{0.3}\text{MnO}_3$ 

Himanshu Jain\*

*Department of Physics, Indian Institute of Science, Bangalore 560 012, India*

A. K. Raychaudhuri†

*S. N. Bose National Centre for Basic Sciences, Salt Lake, Kolkata 700 098, India*

Nilotpal Ghosh‡ and H. L. Bhat

*Department of Physics, Indian Institute of Science, Bangalore 560 012, India*

(Received 16 October 2006; revised manuscript received 7 April 2007; published 10 September 2007)

Colossal electroresistance (CER) has been observed in the ferromagnetic insulating (FMI) state of a manganite. Notably, the CER in the FMI state occurs in the absence of magnetoresistance (MR). Measurements of electroresistance (ER) and current induced resistivity switching have been performed in the ferromagnetic insulating state of a single crystal manganite of composition  $\text{Nd}_{0.7}\text{Pb}_{0.3}\text{MnO}_3$ . The sample has a paramagnetic to ferromagnetic (Curie) transition temperature  $T_C=150$  K and the ferromagnetic insulating state is realized for temperatures  $T\leq 130$  K. The colossal electroresistance, arising from a strongly nonlinear dependence of resistivity ( $\rho$ ) on current density ( $j$ ), attains a large value ( $\approx 100\%$ ) in the ferromagnetic insulating state. The severity of this nonlinear behavior of resistivity at high current densities is progressively enhanced with decreasing temperature, resulting ultimately, in a regime of negative differential resistivity (NDR,  $d\rho/dj < 0$ ) for temperatures  $\leq 25$  K. Concomitant with the buildup of the ER, however, is a collapse of the MR to a small value ( $< 20\%$ ) even in magnetic field,  $H=14$  T. This demonstrates that the mechanisms that give rise to ER and MR are effectively decoupled in the ferromagnetic insulating phase of manganites. We establish that the behavior of ferromagnetic insulating phase is distinct from the ferromagnetic metallic phase as well as the charge ordered insulating phase, which are the two commonly realized ground state phases of manganites.

DOI: [10.1103/PhysRevB.76.104408](https://doi.org/10.1103/PhysRevB.76.104408)

PACS number(s): 75.47.Lx, 75.47.Gk

## I. INTRODUCTION

Electronic transport in hole doped rare earth manganites  $L_{1-x}A_x\text{MnO}_3$  ( $L \equiv \text{Nd, La, Pr}$ ;  $A \equiv \text{Pb, Ca, Sr, Ba}$ ;  $x \leq 0.3$ ) is an issue of current interest since the observation of colossal magnetoresistance (CMR) in this class of materials.<sup>1,2</sup> These materials also exhibit colossal electroresistance (CER), wherein an applied electric field [as in a field effect configuration<sup>3-5</sup>] or an applied current (as in a typical four-probe configuration<sup>6-8</sup>) can change the resistivity ( $\rho$ ) of the sample significantly. Most investigations of CER report a decrease of sample resistivity with increasing sample current. It would be worthwhile to have a clear understanding whether the CER and CMR effects have a common physical origin. We have recently reported that, in at least one system, namely, single crystals of composition  $\text{La}_{0.82}\text{Ca}_{0.18}\text{MnO}_3$ , the CER and CMR phenomena get completely decoupled when the system is in its ferromagnetic insulating (FMI) state.<sup>9</sup> (Note that, by decoupling we mean that a CER is present in the absence of a CMR effect.) In this paper, we report further evidence in favor of different origins of the two phenomena in another and very different manganite system. The system reported in this paper is a single crystal belonging to the family  $\text{Nd}_{1-x}\text{Pb}_x\text{MnO}_3$ .

The phase diagram of the  $\text{Nd}_{1-x}\text{Pb}_x\text{MnO}_3$  system has been studied before and shows that, unlike the  $\text{La}_{1-x}\text{Ca}_x\text{MnO}_3$  system which shows FMI state for  $x \leq 0.18$ , the  $\text{Nd}_{1-x}\text{Pb}_x\text{MnO}_3$  system shows FMI behavior even up to a carrier concentration of  $x \approx 0.3$ .<sup>10</sup> A likely cause of this behavior is the presence of a large disorder due to the very dissimilar ionic sizes of the two ions, Nd and Pb. This disorder can stabilize the insulating state to such high carrier concentration ( $x \approx 0.3$ ).

The effect of disorder in manganites has been investigated extensively and general trends are known. For instance, it has been demonstrated that increasing disorder leads to a metal-insulator transition, i.e., sufficiently high disorder stabilizes an insulating state.<sup>11-14</sup>

The disorder may be quantified as the second moment (variance) of the A-site cation radius distribution,  $\sigma^2 = \sum_i y_i r_i^2 - \langle r_A \rangle^2$ , where  $y_i$  is the fractional substitution level of the  $i$ th A-site species with ionic radius  $r_i$ , and  $\langle r_A \rangle = \sum_i y_i r_i$  represents the average A-site cation radius. As a reference, one needs only to consider the values of disorder in the two prototypical high- $T_C$  manganite compositions [ferromagnetic metallic (FMM) ground state],  $\text{La}_{0.7}\text{Sr}_{0.3}\text{MnO}_3$  ( $T_C \approx 350$  K) (Ref. 15) and  $\text{La}_{0.7}\text{Ca}_{0.3}\text{MnO}_3$  ( $T_C \approx 250$  K) (Ref. 16):  $\sigma^2(\text{La}_{0.7}\text{Sr}_{0.3}\text{MnO}_3) = 1.86 \times 10^{-3} \text{ \AA}^2$ ,  $\sigma^2(\text{La}_{0.7}\text{Ca}_{0.3}\text{MnO}_3) = 2.72 \times 10^{-3} \text{ \AA}^2$  (standard ionic radii were used for these calculations<sup>17</sup>). Compared against these values,  $\sigma^2(\text{Nd}_{0.7}\text{Pb}_{0.3}\text{MnO}_3) = 7.34 \times 10^{-3} \text{ \AA}^2$  is indeed very high. Such a high disorder can localize electrons<sup>12</sup> and destabilize the metallic ground state leading to a ferromagnetic insulating state even at  $x=0.3$ .

The existence of FMI behavior at such a large value of carrier concentration ( $x \approx 0.3$ ) makes  $\text{Nd}_{1-x}\text{Pb}_x\text{MnO}_3$  a very different system from the much studied  $\text{La}_{1-x}\text{Ca}_x\text{MnO}_3$  system; this is apparent from the much reduced resistivity, in the FMI phase, of the composition  $\text{Nd}_{0.7}\text{Pb}_{0.3}\text{MnO}_3$  (NPMO30) as compared against that of the composition  $\text{La}_{0.82}\text{Ca}_{0.18}\text{MnO}_3$  (LCMO18), for instance, the room temperature resistivity of  $\text{La}_{0.82}\text{Ca}_{0.18}\text{MnO}_3$ ,  $\rho_{\text{LCMO18}}(T=300 \text{ K}) = 32 \text{ \Omega cm}$ , which deep in the FMI phase ( $T=55 \text{ K}$ ) grows to  $\rho_{\text{LCMO18}}(T=55 \text{ K}) = 164 \text{ K}\Omega \text{ cm}$ . In con-

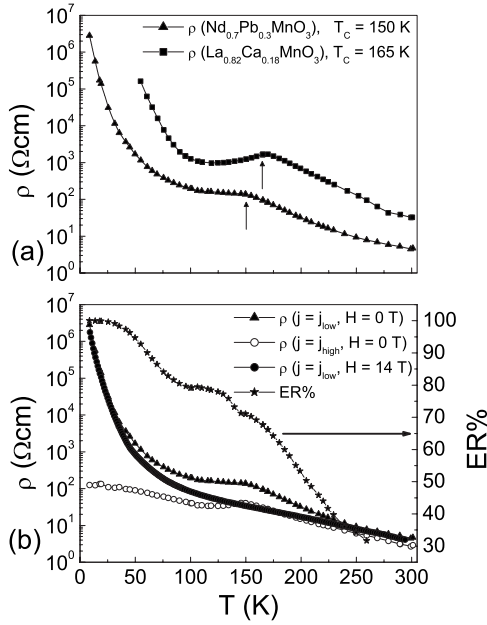


FIG. 1. (a) Comparison of resistivities ( $\rho$ ) of  $\text{Nd}_{0.7}\text{Pb}_{0.3}\text{MnO}_3$  (present investigation) and  $\text{La}_{0.82}\text{Ca}_{0.18}\text{MnO}_3$  (Ref. 9) as a function of temperature ( $T$ ). The paramagnetic to ferromagnetic (Curie) transitions (indicated by arrows) occur at  $T_C = 150\text{ K}$  and  $165\text{ K}$ , respectively. (b) The resistivity vs temperature ( $\rho$ - $T$ ) data of  $\text{Nd}_{0.7}\text{Pb}_{0.3}\text{MnO}_3$  obtained using low bias current density ( $j_{\text{low}}$ ) taken without and with a magnetic field ( $H = 0\text{ T}$  and  $14\text{ T}$ ), and the  $\rho$ - $T$  data taken with high current density ( $j_{\text{high}}$ ) in  $H = 0\text{ T}$ . Electroresistance (ER) as a function of temperature is also plotted ( $\text{ER}\% = 100 \times (\rho(j_{\text{low}}) - \rho(j_{\text{high}})) / \rho(j_{\text{low}})$ ). It may be noted that, for  $T < 100\text{ K}$ , the  $\text{ER} \rightarrow 100\%$ , while the magnetoresistance  $\text{MR} \rightarrow 0\%$ .

trast,  $\text{Nd}_{0.7}\text{Pb}_{0.3}\text{MnO}_3$ , which has a much larger carrier concentration, has  $\rho_{\text{NPMO30}}(T = 300\text{ K}) = 4\text{ }\Omega\text{ cm}$ , and  $\rho_{\text{NPMO30}}(T = 55\text{ K}) = 1.15\text{ K}\Omega\text{ cm}$ . Both the systems, however, despite such large differences in carrier concentration and resistivity undergo the paramagnetic to ferromagnetic (Curie) transition at nearly the same temperature [ $T_C(\text{LCMO18}) = 165\text{ K}$  and  $T_C(\text{NPMO30}) = 150\text{ K}$ ]. Also, the temperatures below which the respective FMI states are realized ( $T_{\text{FMI}}$ ) are nearly the same [ $T_{\text{FMI}}(\text{LCMO18}) \approx 100\text{ K}$  and  $T_{\text{FMI}}(\text{NPMO30}) \approx 130\text{ K}$ ]. To illustrate these aforementioned points, in Fig. 1(a), we show the resistivity ( $\rho$ ) as a function of temperature ( $T$ ) of both systems for comparison; the respective paramagnetic to ferromagnetic (Curie) transitions are indicated by arrows.

In this paper, we report that despite having very different carrier concentration and resistivity as compared to  $\text{La}_{0.82}\text{Ca}_{0.18}\text{MnO}_3$ , the  $\text{Nd}_{0.7}\text{Pb}_{0.3}\text{MnO}_3$  system also shows collapse of magnetoresistance (MR) and a substantial electroresistance (ER) when the system enters the FMI state. This observation thus establishes that the phenomena are general and may indeed be characteristic of the FMI state. We show that in the FMI region ( $T \lesssim 75\text{ K}$ ) the MR essentially collapses to a very small value while the ER reaches its saturation value  $\approx 100\%$ . Furthermore, in this temperature region, the sample shows electric current induced switching

of the resistance state where the resistivity can be switched from a high to a low value by switching the current from a low to a high value. The observation of a CER phenomena in the absence of a CMR also distinguishes the FMI state from a conventional charge ordered insulating (COI) state, which can be destabilized by both current and magnetic fields.<sup>6,18</sup>

We also note that, while electroresistance phenomena in the field effect (FE) geometry have been investigated earlier on the  $L \equiv \text{Nd}$  based family,<sup>19</sup> this paper reports electroresistance due to a current induced field effect in the Nd based manganite.

## II. EXPERIMENTAL DETAILS

The single crystals of composition  $\text{Nd}_{0.7}\text{Pb}_{0.3}\text{MnO}_3$  were grown by the flux-growth technique using  $\text{PbO}/\text{PbF}_2$  solvent. The melt batch was prepared from  $\text{Nd}_2\text{O}_3$ ,  $\text{MnCO}_3$ ,  $\text{PbO}$ , and  $\text{PbF}_2$ . The crystals were grown in Pt crucible with charge to flux ratio of 1:6 and  $\text{PbO}/\text{PbF}_2$  ratio of 1:1.15. The details of growth process have been given elsewhere.<sup>10,20</sup> The crystals used have typical dimensions of  $2 \times 2 \times 3\text{ mm}^3$ . The crystals were characterized by single crystal x-ray diffraction (space group  $P4/mmm$ ) and the composition checked by energy dispersive x-ray analysis and inductively coupled plasma atomic emission spectroscopy.<sup>20</sup>

Measurements of magnetization ( $M$ ) as a function of temperature [zero field cooled (ZFC) and field cooled (FC)] over the magnetic field range,  $H = 10^{-2} - 14\text{ T}$ , and as function of magnetic field up to  $H = 14\text{ T}$  at fixed temperatures, were carried out using a physical property measurement system (PPMS).<sup>21</sup>

Four linear gold contact pads were evaporated onto the crystal and Cu leads (of diameter  $60\text{ }\mu\text{m}$ ) were soldered onto the pads using a Ag-Sn alloy. The experiments were carried out by three methods: (1) by measuring resistance at fixed bias currents as a function of temperature, (2) by taking current-voltage ( $I$ - $V$ ) characteristics at different fixed temperatures, and (3) by measurement of the resistance in response to a two-level current pulse train. While all three methods yield the same data for a given set of parameters, the data reported here were taken mostly by the third method of pulsed current. In this technique, the levels of the high and low current values, the duration of each bias level as well as the number of pulses in the pulse train can be controlled. Most importantly, taking data in pulse mode reduces the effect of Joule heating, if any, to a minimum. It was checked that there was no appreciable heating of the crystal during the measurements. Direct measurement of the rise of sample temperature, by attaching (thermally anchoring) a thermometer directly on top of the crystal, revealed that, for a steady high current bias ( $I_{\text{high}} = 10\text{ mA}$ ), even at the lowest temperature, the rise of sample temperature is below  $4\text{ K}$ , and as the temperature is increased, it is negligible.

The zero-field experiments were carried out in a bath type cryostat. The pulsed bias resistivity measurements were performed by applying a two-level current pulse train to the sample and measuring the resulting voltage output in a standard four-probe geometry. The resistivity measurements at  $14\text{ T}$  were carried out in a PPMS system.<sup>21</sup>

The switching experiment was done by switching the measuring current between a high value and a low value and measuring simultaneously the voltage across the sample, from which the resistance was calculated. The choice of the particular low and high current values was based on measurements of the  $I$ - $V$  characteristics. The low value was chosen to be one within the regime where the sample  $I$ - $V$  characteristics are linear, and the high current value was chosen from within a regime where the  $I$ - $V$  characteristics are strongly nonlinear. The switching time between high and low bias current values was approximately 100  $\mu$ s. In order to record the instantaneous response voltage profile of the sample upon switching the current bias level, the sampling time of each voltage measurement was set at a low value of 20 ms; in addition, no filtering of the sampled data was performed. This enabled us to record correctly the transient response of the sample upon the application of current bias level. Again, at a particular bias level, the response time of the current source (the time required by the instrument to restore the bias to specified fixed value across a changing resistive load) was  $\sim 30$   $\mu$ s, which is 3 orders of magnitude less than the time over which signal is sampled; therefore, from the perspective of measurement considerations, the transient response of the sample is indeed at constant bias (high or low). The (relative) time associated with each voltage measurement was determined via a synchronized oscilloscope with a precision better than 1 ms.

### III. RESULTS AND DISCUSSION

The magnetization ( $M$ ) as a function magnetic field ( $H$ ) at  $T=10$  K up to a magnetic field of 14 T is shown in Fig. 2(a). The apparent lack of any hysteresis confirms that the coercive field is very low ( $\leq 10^{-2}$  T), i.e., NPMO30 is a very soft ferromagnet. The technical saturation is achieved by  $H \approx 1$  T. However, the magnetization does not saturate fully even at a magnetic field as high as 14 T, showing the presence of spin disorder. The high field susceptibility  $\chi_{\text{hf}} = \partial M / \partial H$  as a function of field for  $H > 1$  T is shown in Fig. 2(a) (inset). We note that finite  $\chi_{\text{hf}}$  can also arise from the Nd moments which has been observed before.<sup>23</sup> The spin disorder seen in the high field magnetization likely arises from the large cationic disorder in the system. It has been shown recently, based on magnetization and specific heat measurements, that NPMO30 is a ferromagnet belonging to the three-dimensional-Heisenberg Universality class with short range interactions and that the ferromagnetic transition is continuous.<sup>22</sup> These measurements were based on the same samples as used in the present measurements. To investigate the nature and evolution of the magnetic state of the sample, the magnetization was measured as a function of temperature (ZFC and FC measurements) at both low fields and high fields. In Fig. 2(b), we plot the data from ZFC and FC measurements of  $M$  as a function of  $T$ . It is clear that the sample undergoes a paramagnetic-ferromagnetic (Curie) transition at  $T_C=150$  K. In the low magnetic field data ( $H=10^{-2}$  T,  $5 \times 10^{-2}$  T), the ZFC and FC runs differ although not by a large amount below the Curie temperature ( $T_C$ ). This difference referred to is the signature of some amount of spin

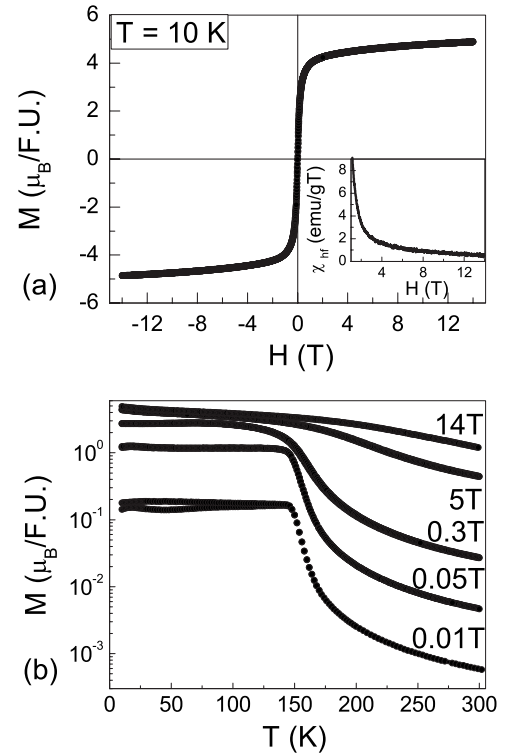


FIG. 2. (a) Magnetization ( $M$ ) vs magnetic field ( $H$ ) loop for  $\text{Nd}_{0.7}\text{Pb}_{0.3}\text{MnO}_3$  at temperature  $T=10$  K. The coercive field  $\leq 10^{-2}$  T. Inset: The high field susceptibility  $\chi_{\text{hf}} = \partial M / \partial H$  for  $H > 1$  T. (b) Magnetization ( $M$ ) as a function of temperature ( $T$ ) for  $\text{Nd}_{0.7}\text{Pb}_{0.3}\text{MnO}_3$  measured at the magnetic fields indicated. The paramagnetic to ferromagnetic (Curie) transition at  $T_C=150$  K is evident. Both zero-field-cooled (ZFC) and field-cooled (FC) measurements were performed.

disorder that is frozen into the ferromagnet order. This is a likely scenario because of the high random disorder ( $\sigma^2$ ) and the competing mixed interactions that are known to be at play in manganite systems. This is especially true for the present sample, being placed, as it is, very close the phase transition boundary between a ferromagnetic metallic and a ferromagnetic insulating ground state.<sup>10</sup> The random field created due to the randomly distributed dopant atoms (Pb) is the factor that contributes to the spin-disorder and irreversibility in the system. The spin disorder in this system is thus a manifestation of the site disorder.<sup>23</sup> The relationship between disorder and formation of polaron in this material is an important issue. For most manganites, as stated earlier, there is indeed a metallic ferromagnetic state at this level of doping. However, in this system, there is formation of an insulating state. It has been shown recently that site disorder can lead to bound polaron formation.<sup>24</sup> As discussed below, formation of bound polaron is needed for the FMI state.

In Fig. 1(b), we show the resistivities ( $\rho$ ) of  $\text{Nd}_{0.7}\text{Pb}_{0.3}\text{MnO}_3$  as a function of temperature ( $T$ ) measured with two current densities ( $j$ ) in the absence of magnetic field ( $H=0$  T). The data were taken with current density,  $j = j_{\text{low}} \approx 6.7 \times 10^{-4}$  A/cm<sup>2</sup> (corresponding to a sample current,  $I_{\text{low}}=10$   $\mu$ A). At this value of  $j$ , the  $\rho$  is independent of the measuring current density. The  $\rho$  exhibits a peak at  $T_p$

$\approx 150$  K below which the sample enters a FMM phase.

This FMM phase, however, appears to be highly resistive and percolative in character. The behavior in this phase, of the  $\rho$ - $T$  curve, suggests that the FMM phase may be coexistent with an insulating phase. The  $\rho$  shows a small drop until  $T \approx 130$  K, and below this temperature, with onset of the FMI phase, it increases rapidly following a Mott variable range hopping relation<sup>25</sup> for  $T \lesssim 75$  K. In Fig. 1(b), we also show the data taken using a high bias current density,  $j_{\text{high}} \approx 6.7 \times 10^{-1}$  A/cm<sup>2</sup> (corresponding to a current,  $I_{\text{high}} = 10$  mA). It is evident that there is a significant decrease in  $\rho$  due to the (high) applied current. This current induced suppression of the resistivity is progressively enhanced as the temperature decreases, and at the lowest temperature measured,  $\rho(j_{\text{high}})/\rho(j_{\text{low}}) < 5 \times 10^{-5}$ .

In Fig. 1(b), we also show the most important observation of the present investigation. Here, alongside the aforementioned low current zero magnetic field data, we show the  $\rho$  measured using low current density ( $j_{\text{low}}$ ) in a magnetic field,  $H=14$  T. It is clear that there is substantial MR in the temperature range 65–225 K (attaining its highest value of  $\approx 80\%$  at  $T_p \approx 150$  K just as in other CMR single crystalline materials).<sup>1,2</sup> Furthermore, as temperature decreases, the sample enters the FMI state at  $T_{\text{FMI}} \approx 130$  K and the MR, even at a field of 14 T, becomes very small ( $\leq 20\%$ ) below 75 K. The above observation is to be compared with the effect, on the sample, of a large bias current density: comparing this  $\rho$ - $T$  data taken in a magnetic field to the  $\rho$ - $T$  data measured at high current density ( $j_{\text{high}}$ ) makes evident that, while the magnetic field has a negligible effect on the resistivity, the current induces a substantial (4 orders of magnitude) depression of resistivity ( $\rho$ ). In Fig. 1(b), we also plot the ER defined as

$$\text{ER \%}(T) = 100 \times \frac{\rho(j_{\text{low}}) - \rho(j_{\text{high}})}{\rho(j_{\text{low}})}(T) \quad (1)$$

as a function of temperature (right y axis). It can be seen that, when the MR collapses in the FMI phase ( $T \lesssim 75$  K), the ER picks up reaching a value of nearly 100% at the lowest temperature. This experiment thus demonstrates that there is an effective decoupling of the mechanism of ER and that of MR in the FMI phase. This result is rather distinct from previous results that used compositions in the FMM<sup>4</sup> phase or COI<sup>6,18</sup> phase. Our observation, then, distinguishes the FMI state from the COI state. The former can be destabilized, to a more conducting state, only by a current, while the latter can be destabilized by both current and magnetic fields. The CER nevertheless, is a feature of the FMI state as well as of the COI state.

To test the possibility of Joule heating being responsible for the above effect, we took data using the pulsed current technique, by varying the duty cycle. The results, shown in Fig. 4 (inset), are independent of the duty cycle. For instance, at  $T=40$  K, by varying the high current “on” time from 1 to 100 s (i.e., over 2 orders of magnitude), the measured resistivity changed by  $< 0.5\%$ , thus ruling out any significant sample heating, at least down to  $T=40$  K. Also, as has already been mentioned, the sample temperature rise (at

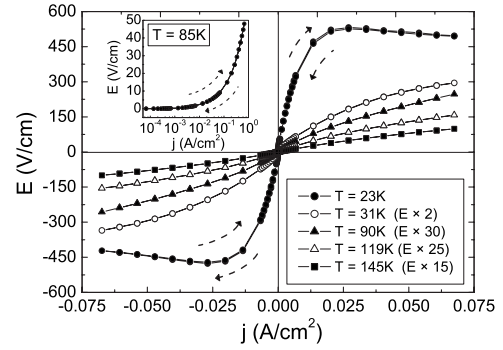


FIG. 3. Current vs voltage ( $I$ - $V$ ) characteristics of  $\text{Nd}_{0.7}\text{Pb}_{0.3}\text{MnO}_3$  at few representative temperatures ( $T$ ) as indicated [the data are plotted in specific units as current density vs electric field ( $j$ - $E$ )]. A representative semilog plot in inset demonstrates the absence of hysteresis in  $j$ - $E$  characteristics over 4 orders of magnitude variation in  $j$ . The  $T=23$  K  $j$ - $E$  characteristic exhibiting the negative differential resistivity (NDR) feature is noteworthy. (Note the scaling of  $E$  by the numerical factors mentioned in parentheses.)

the lowest measured temperature) due to passage of high bias current ( $I_{\text{high}}=10$  mA), as measured by directly attaching a thermometer on top of the sample, was estimated to be  $< 4$  K.

In Fig. 3, we show the current vs voltage ( $I$ - $V$ ) characteristics taken on the sample at different temperatures [the data are rendered independent of particular sample dimensions by plotting it in specific units as current density vs electric field ( $j$ - $E$ )]. The nonlinear nature of the transport is clearly evident, and the data reveal a continuous decrease in  $\rho(=E/j)$  as  $j$  increases. The nonlinearity becomes progressively more severe with decreasing temperature. In fact, for  $T \lesssim 25$  K, the  $j$ - $E$  curve shows a region of negative differential resistivity (NDR) where  $dE/dj < 0$ . We have reported earlier such a NDR effect in a single crystal COI sample of composition  $\text{Pr}_{0.63}\text{Ca}_{0.37}\text{MnO}_3$ .<sup>18,26</sup> Occurrence of such a NDR effect has also been reported in COI state of thin film  $\text{Nd}_{0.5}\text{Ca}_{0.5}\text{MnO}_3$ .<sup>27</sup> Here we report NDR in the FMI state. At present, however, there is no clear understanding of the NDR phenomena.

A notable feature of the data is the absence of hysteresis in the  $I$ - $V$  ( $j$ - $E$ ) curves shown in Fig. 3. This is further evidence distinguishing the FMI state from the charge ordered (CO) state. This is so because, a CO state is characterized by a strong hysteresis in the  $j$ - $E$  characteristics.<sup>18</sup> The hysteretic  $j$ - $E$  curve in COI materials is often interpreted as a signature of electronic phase separation. It arises due to the kinetic effect, as determined by the potential barrier that separates the phases. Based on this observation of nonhysteretic  $j$ - $E$  characteristics in the FMI state, we suggest that, whatever may be the underlying natures of the phases comprising the phase-separated state, the potential barrier between them is low enough to have precluded the observation of any substantial kinetic effects in the time window of the present measurements.

In Fig. 4, we show the representative data (at  $T=55$  K) of variation of resistivity ( $\rho$ ) as a function of current density ( $j$ ), plotted in a log-log (base 10) scale. It is clear that there exists

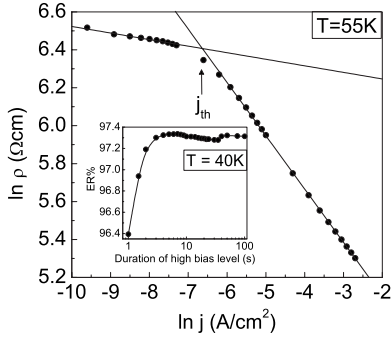


FIG. 4. A representative log-log plot showing two regimes of power law variation of resistivity ( $\rho$ ) as a function of bias current density ( $j$ ) at temperature,  $T=55$  K. The threshold current density ( $j_{th}$ ) is indicated. The lines are least squares best fits in the two regimes. Such analysis was used to obtain the parameters— $\alpha_1$ ,  $\alpha_2$ ,  $m_1$ ,  $m_2$ —as are plotted in Fig. 5. Inset: Absence of any substantial variation of electroresistance (ER) as the duration of high current bias level is changed in a typical pulsed current experiment.

a threshold current density ( $j_{th}$ , indicated by an arrow) that separates two distinct  $\rho$ - $j$  regimes, and that, in both regimes, the dependence of  $\rho$  on  $j$  is a power law. Below the threshold current, i.e.,  $j < j_{th}$ ,  $\rho$  is weakly dependent on  $j$  and in this region  $\rho \propto j^{m_1}$ , with  $m_1$  close to zero. However, for  $j > j_{th}$ , a strong nonlinear regime sets in, and  $\rho$  decreases strongly with increasing  $j$ .

The  $\rho$ - $j$  datasets then, taken at fixed temperatures, may be fitted to the relation

$$\rho = \alpha_n j^{m_n}, \quad (2)$$

where the subscripts  $n=1$  and 2 denote the regimes  $j < j_{th}$  and  $j > j_{th}$ , respectively. The thus obtained exponents  $m_1$  and  $m_2$  and the coefficients  $\alpha_1$  and  $\alpha_2$  are plotted in Fig. 5 as a function of temperature ( $T$ ). The systematic development of the nonlinear effects and the strong current dependence of the resistivity (which gives the CER) in the low temperature FMI phase is evident. The CER is related to the strong nonlinear component that appears beyond the threshold current density  $j_{th}$ . It is evident from Figs. 5(a)–5(d) that the nonlinear conductivity, as measured by  $|m_2|$  and  $\alpha_2$  increases sharply at  $T \approx 38$  K. In fact,  $m_1$  and  $\alpha_1$  also show a marked change at this temperature. In Fig. 5(e), we show the variation of the threshold current density ( $j_{th}$ ) as a function of temperature ( $T$ ). It can be seen that, while  $j_{th}$  has a shallow  $T$  dependence above  $T=38$  K (decreasing with decreasing temperature), there is a prominent jump, followed by a rapid drop below this temperature. In fact, all the parameters— $\alpha_1$ ,  $\alpha_2$ ,  $m_1$ ,  $m_2$ —exhibit an anomaly at this temperature. It is suspected that this sharp anomaly may be caused by a phase transition type of phenomena setting in at  $T \approx 38$  K. Detailed investigation of this is underway. The NDR seen in the  $j$ - $E$  curves at low temperatures (see Fig. 3) typically appears after the system has undergone this transition.

In Fig. 6, we show representative current induced resistivity switching data. Figure 6(a) shows the data at a temperature when the sample has just entered the FMI state ( $T=130$  K) and Fig. 6(b) shows the data when the sample is

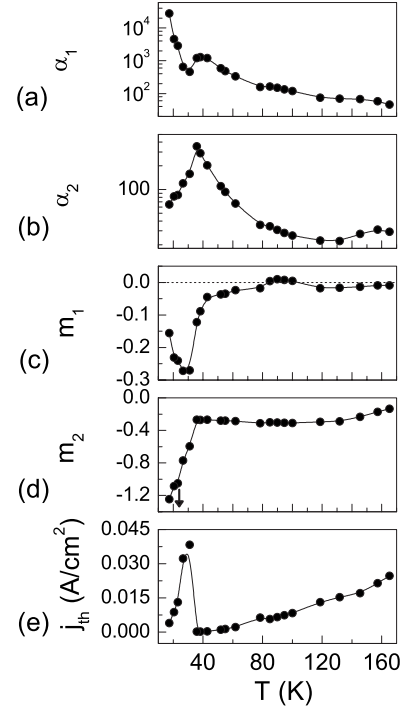


FIG. 5. Variation of (a)  $\alpha_1$ , (b)  $\alpha_2$ , (c)  $m_1$ , (d)  $m_2$ , and (e)  $j_{th}$  as a function of temperature ( $T$ ) in the ferromagnetic insulating state. One may notice the rapid decrease in  $m_2$  for  $T \lesssim 38$  K. The negative differential resistivity (NDR) regime ( $m_2 < -1$ ) is realized for  $T \lesssim 25$  K [indicated by arrow in (d)]. See also Eq. (2) and Fig. 3.

deep into the FMI state ( $T=42$  K). The switching of the resistance follows the switching of the current with a small drag of  $\approx 2-3$  s, following which the full time independent value of ER [as plotted in Fig. 1(b)] is realized. This rules out sample heating as that would have caused a change in the ER (as the sample heats up).

The switching phenomena seen in the FMI samples are strong manifestations of the CER effect. The switching data show that the resistance of the sample follows the measuring current (almost) without any lag. This rules out any significant capacitive or charge storage effect, as that would have caused the voltage rise to lag behind the current.

#### IV. CONCLUSIONS

In the present investigation, we establish that it is possible to have a very large (colossal) electroresistance (CER) in the absence of a substantial magnetoresistance (MR) at least in one type of manganites, namely, those that exhibit a low temperature ferromagnetic insulating (FMI) phase. We have observed this in two widely differing samples:  $\text{Nd}_{0.7}\text{Pb}_{0.3}\text{MnO}_3$  (present investigation) and  $\text{La}_{0.82}\text{Ca}_{0.18}\text{MnO}_3$ .<sup>9</sup> This is intelligible proof that the origin of the two phenomena of CER and CMR can be different.

We also note the distinct nature of the FMI phase. This phase is interesting because, in a double-exchange system, ferromagnetism is always associated with a metal-like ( $dp/dT > 0$ ) behavior. If the FMI phase is explained as a phase-separated state consisting of a FMM phase and a para-

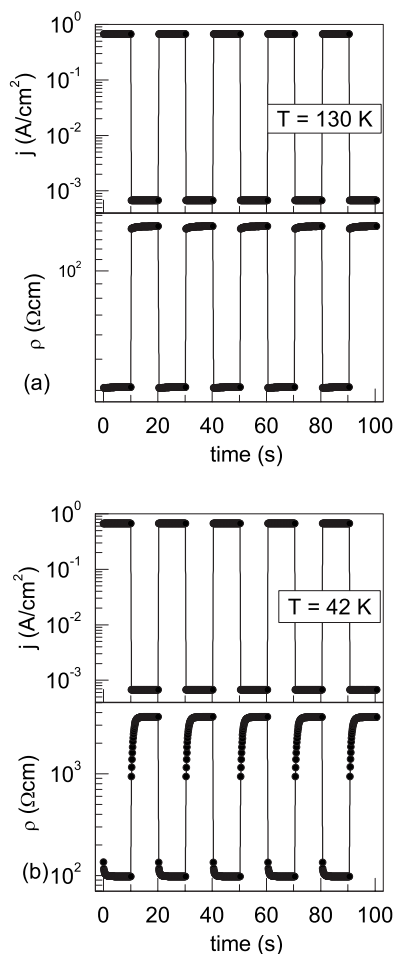


FIG. 6. Representative datasets showing switching of resistivity ( $\rho$ ) upon application of a current density ( $j$ ) pulse train at (a)  $T = 130$  K, just within the ferromagnetic insulating (FMI) state, and (b)  $T = 42$  K, deep in the FMI state.

magnetic insulating phase with the FMM phase fraction below the percolation threshold, then one may still explain the FMI phase within the framework of the double-exchange mechanism. The volume fraction of the insulating phase being in majority results in the material being insulating. The passage of current destabilizes the insulating phase making it more metallic; this increase in the volume of the metallic phase reduces the resistivity. This scenario is distinct from the formation of ferromagnetic metallic filaments as has been seen in charge ordered insulating (COI) state.<sup>26,28</sup> However, such percolation based model is incompatible with the nearly full saturation magnetization of  $3.8\mu_B$  per formula unit,<sup>23</sup> as has been observed in these systems. With such a moment, it is difficult to justify that the FMM phase is in minority. The quandary arises from the nature of the insulating phase. As has been pointed out in the previous section, this (colossal) ER is a feature of the COI state as well. However, the absence of any substantial MR suggests that the insulating nature of the FMI phase is distinct from that of COI phases.<sup>18</sup>

It needs to be pointed out, however, that there is little quantitative theoretical understanding of the FMI phase. The current paradigm of CMR manganite physics is based on the

double-exchange (DE) mechanism of ferromagnetism, which, however, does not allow for a state that is simultaneously ferromagnetic and insulating. In this model, the ferromagnetic exchange is due to mobile holes. Theoretical studies have investigated the localization properties induced by disorder within the DE model.<sup>29</sup> The studies concluded that the fraction of the localized state is very small so that the insulating state is not possible. A more recent study<sup>30</sup> has proposed a virtual DE model in which one does not need mobile holes for ferromagnetism. In this model, which is a two fluid model, two distinct types of carriers are present in the system, namely, Jahn-Teller polarons ( $l$ ) that are essentially site localized, and band electrons ( $b$ ) that can hop between sites in the random medium. The ferromagnetism in this virtual DE model needs coexisting Jahn-Teller polaron and holes. In this model, depending on the relative strength of the Jahn-Teller energy ( $E_{JT}$ ) and the bandwidth ( $D_0$ ), the ferromagnetic state appears beyond a certain hole concentration. The resulting state is metallic if the bandwidth is large, so that bottom of the band of mobile carriers ( $b$ ) is pulled below the chemical potential. For lower bandwidth, it has been shown<sup>30,31</sup> that there exists a ferromagnetic virtual DE process in which the holes and the JT polarons can both be site localized, leading to an insulating state. The existence of the insulating or the metallic state thus depends on the relative strengths of  $E_{JT}$  and  $D_0$  and not on the spin ordering as is required by the conventional DE model. A calculation<sup>31</sup> based on this model showed that larger  $D_0$  and thus a smaller value of the ratio  $E_{JT}/D_0$  will reduce the resistivity by populating more carriers in the mobile band  $b$  and can even drive the system metallic. In this model there exist distinct FMM and FMI phases as a function of  $D_0$ . We note that based on this model, any mechanism that enhances  $D_0$  will thus reduce the resistivity. For FMI materials, a likely cause of the destabilization of the insulating phase can be a current induced enhancement of transfer integral between the electrons of neighboring  $e_g$  orbitals that form the conduction band. In recent years, a number of theories have been proposed where the spin alignment or transfer by a current have been envisaged.<sup>32-34</sup> The important outcome from these theories is that a large current can enhance the hopping integral. Though applicability of such ideas has not been explored in detail for manganite systems, one may propose a simple scenario based on such ideas. We propose that an enhanced current, in excess of what a simple equilibrium situation would allow, will enhance the transfer integral. This in turn will enhance the bandwidth  $D_0$ . A decreased  $E_{JT}/D_0$  ratio will lead to a suppression of resistivity. In such a scenario, the CER and current induced switching can occur by an enhanced current density and it can indeed be delinked from the CMR phenomena.

In summary, the present investigation has established two noteworthy and distinctive features of ferromagnetic insulating (FMI) phase of colossal magnetoresistive (CMR) manganites. First, that the FMI phase shows no MR although it shows a CER. The CER is associated with strong nonlinear conductivity effects such as current induced resistivity switching as well as negative differential resistivity. This observation points to different origins for the two phenomena of CER and CMR. Second, the FMI phase, as an insulating

state, is distinct from the COI state which can be destabilized by both a magnetic field and an electric field, unlike the FMI phase.

#### ACKNOWLEDGMENTS

One of the authors (H.J.) thanks the Council of Scientific

and Industrial Research (CSIR), India, for support. Another author (A.K.R.) thanks the Department of Science and Technology (DST), India, for a sponsored project. Part of this work was performed at the National Low Temperature Facility at UGC-DAE Consortium for Scientific Research, Indore. The authors thank Alok Banerjee and V. Ganesan for making available their PPMS facilities.

\*himanshu@physics.iisc.ernet.in

†Present address: Universität Leipzig, Fakultät für Physik und Geowissenschaften, Institut für Experimentell Physik II, Technicum Analyticum, Linne Strasse-3-5, 04103 Leipzig, Germany.

‡On leave from Department of Physics, Indian Institute of Science, Bangalore 560 012, India; arup@bose.res.in

<sup>1</sup>*Colossal Magnetoresistance, Charge Ordering and Related Properties of Manganese Oxides*, edited by C. N. R. Rao and B. Raveau (World Scientific, Singapore, 1998).

<sup>2</sup>*Colossal Magnetoresistive Oxides*, edited by Y. Tokura (Gordon and Breach, London 2000); Y. Tokura, Rep. Prog. Phys. **69**, 797 (2006).

<sup>3</sup>T. Zhao, S. B. Ogale, S. R. Shinde, R. Ramesh, R. Droopad, J. Yu, K. Eisenbeiser, and J. Misewich, Appl. Phys. Lett. **84**, 750 (2004); X. P. Zhang, B. T. Xie, Y. S. Xiao, B. Yang, P. L. Lang, and Y. G. Zhao, *ibid.* **87**, 072506 (2005).

<sup>4</sup>T. Wu, S. B. Ogale, J. E. Garrison, B. Nagaraj, Amlan Biswas, Z. Chen, R. L. Greene, R. Ramesh, T. Venkatesan, and A. J. Millis, Phys. Rev. Lett. **86**, 5998 (2001).

<sup>5</sup>A. Odagawa, H. Sato, I. H. Inoue, H. Akoh, M. Kawasaki, Y. Tokura, T. Kanno, and H. Adachi, Phys. Rev. B **70**, 224403 (2004).

<sup>6</sup>A. Asamitsu, Y. Tomioka, H. Kuwahara, and Y. Tokura, Nature (London) **388**, 50 (1997).

<sup>7</sup>A. K. Debnath and J. G. Lin, Phys. Rev. B **67**, 064412 (2003).

<sup>8</sup>Y. G. Zhao, Y. H. Wang, G. M. Zhang, B. Zhang, X. P. Zhang, C. X. Yang, P. L. Lang, M. H. Zhu, and P. C. Guan, Appl. Phys. Lett. **86**, 122502 (2005).

<sup>9</sup>Himanshu Jain, A. K. Raychaudhuri, Ya. M. Mukovskii, and D. Shulyatev, Appl. Phys. Lett. **89**, 152116 (2006).

<sup>10</sup>Nilotpal Ghosh, Suja Elizabeth, H. L. Bhat, and P. L. Paulose, J. Appl. Phys. **96**, 3343 (2004).

<sup>11</sup>K. F. Wang, Y. Wang, L. F. Wang, S. Dong, D. Li, Z. D. Zhang, H. Yu, Q. C. Li, and J. -M. Liu, Phys. Rev. B **73**, 134411 (2006).

<sup>12</sup>K. F. Wang, F. Yuan, S. Dong, D. Li, Z. D. Zhang, Z. F. Ren, and J. -M. Liu, Appl. Phys. Lett. **89**, 222505 (2006).

<sup>13</sup>A. Maignan, C. Martin, G. Van Tendeloo, M. Hervieu, and B. Raveau, Phys. Rev. B **60**, 15214 (1999).

<sup>14</sup>J. A. Souza and R. F. Jardim, Phys. Rev. B **71**, 054404 (2005).

<sup>15</sup>K. Ghosh, C. J. Lobb, R. L. Greene, S. G. Karabashev, D. A.

Shulyatev, A. A. Arsenov, and Y. Mukovskii, Phys. Rev. Lett. **81**, 4740 (1998).

<sup>16</sup>J. Mitra, A. K. Raychaudhuri, Ya. M. Mukovskii, and D. Shulyatev, Phys. Rev. B **68**, 134428 (2003).

<sup>17</sup>R. D. Shannon, Acta Crystallogr., Sect. A: Cryst. Phys., Diffr., Theor. Gen. Crystallogr. **32**, 751 (1976).

<sup>18</sup>Ayan Guha, A. K. Raychaudhuri, A. R. Raju, and C. N. R. Rao, Phys. Rev. B **62**, 5320 (2000).

<sup>19</sup>S. B. Ogale, V. Talyansky, C. H. Chen, R. Ramesh, R. L. Greene, and T. Venkatesan, Phys. Rev. Lett. **77**, 1159 (1996).

<sup>20</sup>Nilotpal Ghosh, Suja Elizabeth, H. L. Bhat, G. N. Subanna, and M. Sahana, J. Magn. Magn. Mater. **256**, 286 (2003).

<sup>21</sup>Quantum Design, 6325 Lusk Boulevard, San Diego, CA 92121-3733.

<sup>22</sup>Nilotpal Ghosh, S. Rößler, U. K. Rößler, K. Nenkov, S. Elizabeth, H. L. Bhat, K. Dörr, and K.-H. Müller, J. Phys.: Condens. Matter **18**, 557 (2006).

<sup>23</sup>Nilotpal Ghosh, Suja Elizabeth, H. L. Bhat, U. K. Rößler, K. Nenkov, S. Rößler, K. Dörr, and K.-H. Müller, Phys. Rev. B **70**, 184436 (2004).

<sup>24</sup>Sanjeev Kumar and Pinaki Majumdar, Phys. Rev. Lett. **96**, 016602 (2006).

<sup>25</sup>N. F. Mott, *Conduction in Non-Crystalline Materials*, 2nd ed. (Clarendon Press, Oxford, 1993).

<sup>26</sup>Ayan Guha, N. Khare, A. K. Raychaudhuri, and C. N. R. Rao, Phys. Rev. B **62**, R11941 (2000).

<sup>27</sup>Ayan Guha, Arindam Ghosh, A. K. Raychaudhuri, S. Parashar, A. R. Raju, and C. N. R. Rao, Appl. Phys. Lett. **75**, 3381 (1999).

<sup>28</sup>Manfred Fiebig, Kenjiro Miyano, Yoshinori Tomioka, and Yasuhide Tokura, Science **280**, 1925 (1998).

<sup>29</sup>Qiming Li, Jun Zang, A. R. Bishop, and C. M. Soukoulis, Phys. Rev. B **56**, 4541 (1997).

<sup>30</sup>T. V. Ramakrishnan, H. R. Krishnamurthy, S. R. Hassan, and G. Venketeswara Pai, Phys. Rev. Lett. **92**, 157203 (2004).

<sup>31</sup>T. V. Ramakrishnan, J. Phys.: Condens. Matter **19**, 125211 (2007).

<sup>32</sup>L. Berger, Phys. Rev. B **54**, 9353 (1996).

<sup>33</sup>J. C. Slonczewski, J. Magn. Magn. Mater. **159**, L1 (1996).

<sup>34</sup>L. Berger, J. Appl. Phys. **89**, 5521 (2001).